Comparing a topological local state and a defect induced local state in metamaterials

Written by: Lior Moneta & Shira Tal

Under the guidance of Tom Dvir

Topological states are of great interest especially for their possible applications in quantum computing. Following previous work on topological states in CRLH transmission lines, it was shown that it is possible to map Dirac's equation in 1D to Maxwell's equations. Thus, enabling measurement of small-scale physical phenomena using electromagnetic waves and systems. In this experiment we use CRLH TL to simulate lines with different masses. We reproduce a previously accomplished experiment and create a local topological state in the boundary of two masses metamaterial. We then compare its behavior to that of a defect induced local state in a single mass metamaterial. We show that both of these states act similarly locally and over the entire line and may be hard to distinguish from one another using the measurements we applied. Finally, we suggest further experiments to help differentiate between the two, and also start exploring the stability of topological states in the presence of defects.

We wish to thank Tom Dvir for the guidance, Prof. Nadav Katz for supporting this experiment and for supplying with the infrastructure and the facilities for the experiment, Lior Oppenheim and Yoav Rubinstein for their previous work [1] on this experiment which enabled our work, and for their advice and help on the measurement systems and simulations.

Table of Contents

Introduction:

Topological states are of great interest especially for their possible applications in quantum computing. Following previous work [1] [2] on topological states in CRLH transmission lines, it was shown that it is possible to map Dirac's equation in 1D to Maxwell's equations. Thus, enabling measurement of small-scale physical phenomena using electromagnetic waves and systems. This mapping is provided by the following defenitions:

$$(1)\ \phi = \begin{pmatrix} \sqrt{\epsilon_0} E_z \\ \sqrt{\mu_0} H_y \end{pmatrix}$$

$$(2)\ V(x) = \frac{\omega}{2c}[\epsilon_r(x) + \mu_r(x) - \langle \epsilon_r(x) + \mu_r(x) \rangle]$$

$$(3)\ E = -\frac{\omega}{2c}\langle \epsilon_r(x) + \mu_r(x) \rangle$$

$$(4)\ m(x) = \frac{\omega}{2c}[\epsilon_r(x) + \mu_r(x)]$$

Using equation 1-4 one can map Maxwell's equation to Dirac' equation:

$$(5)\ \begin{cases} -\partial_x E_z = i\omega\mu_0\mu_r(x) H_y \\ \partial_x H_y = -i\omega\epsilon_0\epsilon_r(x) E_z \end{cases} \Leftrightarrow [-i\sigma_x\partial_x + m(x)\sigma_z + V(x)]\phi = E\phi$$

This mapping enables to model any mass and potential in Dirac's equation by controlling the permittivity and permeability along a line. This is achieved by building metamaterials which enable the engineering of those parameters.

Using this mapping and the ability to engineer parameters of the line we explore the phenomena happening at the boundary of positive and negative masses line. We first validate our ability to simulate this type of systems using ABCD matrices by testing them on a simple filter made of two types of coplanar waveguides. Then using a single mass line, made of a CRLH circuit on top of a CPW we further validate our ability to predict characteristics of those systems such as the band gap, the transfer coefficient and the dispersion relation. Finally, we explore the similarities and differences between a topological state created in the boundary between 2 opposite sign masses line and a defect induced local state in a one mass metamaterial line.

For all of these systems we measure the transfer coefficient and scan the wave function along the line. We compare our experimental results to numerical results and extend our work with simulations where experimental work was not possible in the resource and time frame of this experiment. Finally, we conclude and give an outlook to further experiments to be made using our system and similar systems.

Theoretical Background

Transmission lines:

In order to understand the system we built it is important to first talk about transmission lines (TL). A TL is usually schematically represented as a two-wire line (one conducting and the other grounded), since TL for traverse electromagnetic wave propagation (TEM) consists at least two conductors.

An infinitesimal piece of the line with length dx can be modeled by discrete element circuit, as shown in Fig1, where R, L, G, and C are per unit length quantities. These quantities are defined as follows:

R = series resistance per unit length in $\left[\frac{\Omega}{m}\right]$.

L = series inductance per unit length in $\left[\frac{H}{m}\right]$.

G = shunt conductance per unit length in $\left[\frac{S}{m}\right]$.

C = shut capacitance per unit length in $\left[\frac{F}{m}\right]$.

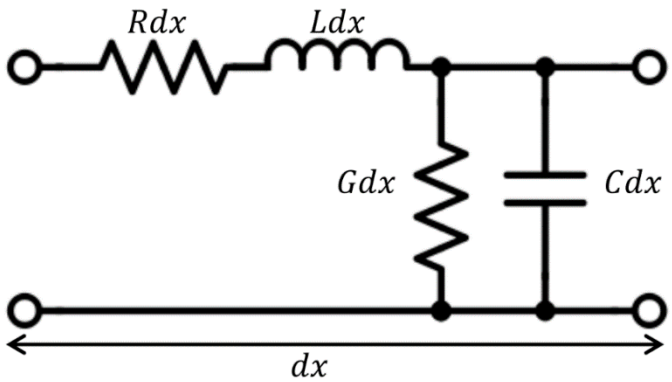

Figure 1 – Model of a circuit TL for a discrete unit length dx.

Using Kirchhoff's laws one can reach the telegrapher's equations and from their solution deduce the complex propagation constant γ and the characteristic impedance of the TL Z_0 [3, pp. 50-51].

$$(6)\ Z_0 = \sqrt{\frac{R + i\omega L}{G + i\omega C}}$$

$$(7)\ \gamma = \alpha + i\beta = \sqrt{(R + i\omega L)(G + i\omega C)}$$

And for an ideal lossless TL (R = G = 0), $\alpha = 0$; $\beta = \omega\sqrt{LC}$ and $Z_0 = \sqrt{\frac{L}{C}}$. Using Maxwell's equations, we can get a connection to the parameters of the material such as the effective permeability ϵ_r and the effective permittivity μ_r:

$$(8a)\ \epsilon_r = C \cdot p$$

$$(8b)\ \mu_r = \frac{L}{p}$$

Where p is the form factor derived from the geometry of the waveguide.

Composite Right Left Hand TL

Metamaterials are materials that can be engineered to have unnatural properties, such as negative mass and negative permeability and permittivity. In natural systems, electromagnetic waves travel through the media with right-hand chirality, which means the pointing vector ($\vec{E} \times \vec{B}$) is in the direction of the wave's propagation. Composite right left hand (CRLH) system exhibit also the opposite behavior, having a left-hand chirality and the pointing vector in the opposite direction. The latter happens in systems that possess negative permeability and permittivity ($\epsilon_r, \mu_r < 0$). Such a systems can be obtained by soldering series capacitors and shunt inductors on a regular TL. As before it can be schematically represented by two lines, the TL is assembled from discrete TL of length d (unit cells) that are connected by series capacitors (C_s) and are grounded by one or more shunt inductors (L_s), as can be seen in Fig2.

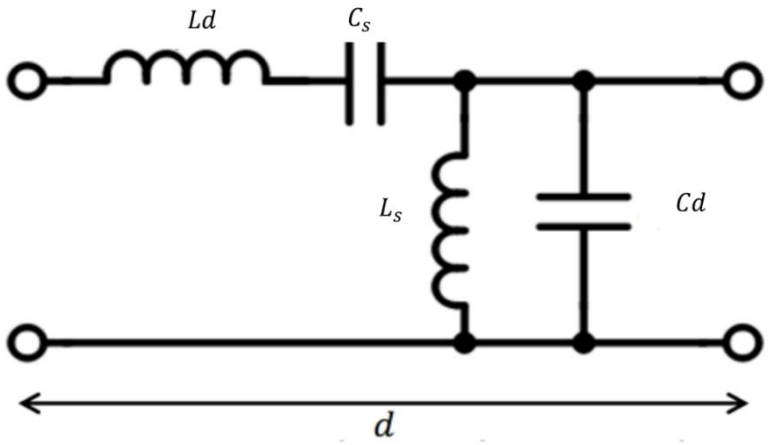

Figure 2 – Circuit model of a lossless CRLH unit cell of length d.

For such a model the propagation factor and the characteristic impedance are as follows [4]:

$$(9)\ \gamma = i\omega\sqrt{\left(L - \frac{1}{\omega^2 C_s d}\right)\left(C - \frac{1}{\omega^2 L_S d}\right)}$$

$$(10)\ Z_0 = \sqrt{\frac{L - \frac{1}{\omega^2 C_s d}}{C - \frac{1}{\omega^2 L_S d}}}$$

And the effective permittivity and permeability are as well:

$$(11a)\ \epsilon_r = \frac{1}{p\epsilon_0}\left(C - \frac{1}{\omega^2 L_s d}\right)$$

$$(11b)\ \mu_r = \frac{p}{\mu_0}\left(L - \frac{1}{\omega^2 C_s d}\right)$$

From (11a) and (11b) one can deduce the conditions for left or right hand chirality, first we shall define the border line where $\mu_r = \epsilon_r = 0$:

$$(12a)\ \omega_1 = \frac{1}{\sqrt{L_s C d}}$$

$$(12b)\ \omega_2 = \frac{1}{\sqrt{LC_s d}}$$

For right hand chirality $\omega < \omega_1, \omega_2$ and for left hand chirality $\omega > \omega_1, \omega_2$ otherwise we get a band gap. This corresponds directly with Dirac's equation, a metamaterial with $\omega_1 > \omega_2$ will have negative mass ($\mu(\omega) > \epsilon(\omega)$ equation (4)) and the opposite ($\omega_1 < \omega_2$) for positive mass. Note that due to this topological difference, it is impossible not to pass through zero mass when moving from one metamaterial with negative mass to another with positive mass or vice versa.

ABCD matrices

ABCD matrices represent the linear relation between the voltage and current between two ports in a network see Fig3. For more than two ports these matrices can be multiplied, so in the case of a TL of

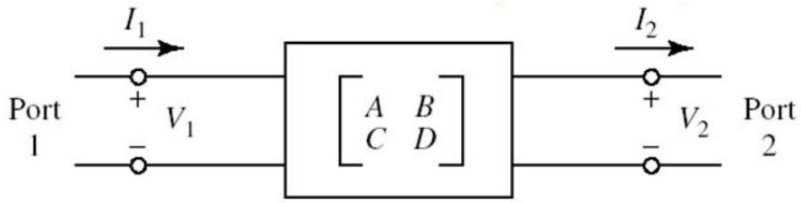

Figure 3 – A two port network represented by an ABCD matrix.

N ports we can calculate an ABCD matrix that represents the current and voltage at the first and last ports of the line. These matrices were used to simulate the system, there are different matrices for different components as follows [3, p. 185]:

Table 1 – ABCD matrices that were used during the experiment for simulations

Type	Schema	Matrix
Series element of impedance Z	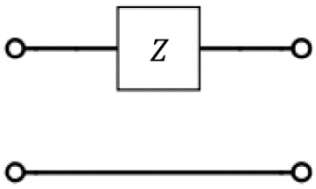	$\begin{bmatrix} 1 & Z \\ 0 & 1 \end{bmatrix}$
Shunt elements of impedance Z	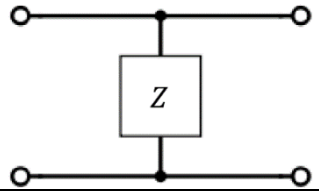	$\begin{bmatrix} 1 & 0 \\ \frac{1}{Z} & 1 \end{bmatrix}$
Transmission line of length l	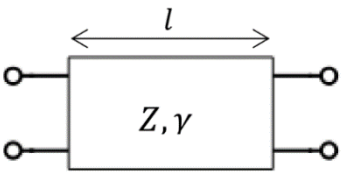	$\begin{bmatrix} \cosh(\gamma l) & Z\sinh(\gamma l) \\ \frac{1}{Z}\sinh(\gamma l) & \cosh(\gamma l) \end{bmatrix}$

Microwave filters

It is possible to build a band-stop filter by connecting infinite units of two alternating TL of length l with different characteristic impedances Z_1, Z_2 and different propagation constants γ_1, γ_2, using the theory mentioned above of ABCD matrices one can prove this claim.

We are able to produce an analytical solution to this kind of TL using the concept of Bloch waves. The TL is modeled as a one-dimensional endless chain of unit cells (each consists of two different TL), therefor a steady solution $\psi(x)$ of the Bloch wave is assumed:

$$(13)\ \psi(x) = e^{-\gamma x}u(x)$$

Where $u(x)$ is periodic with the period of the unit cell. Again γ is purely imaginary, $\gamma = \alpha + i\beta$, and we can reach the following connection between γ and γ_1, γ_2 Invalid source specified.:

$$(14)\ \cosh(2\gamma l) = \cos(\beta_1 l)\cos(\beta_2 l) - \frac{1}{2}\sin(\beta_1 l)\sin(\beta_2 l)\left(\frac{Z_1^2 + Z_2^2}{Z_1 Z_2}\right)$$

Solutions for equation (14) exist only if either $\alpha = 0$ or $\beta = 0$ because the RHS is always real.
For the case $\alpha = 0 \ \Rightarrow \ \gamma = i\beta$ we get $\cosh(2\gamma l) = \cos(2\beta l)$, since cosine is bounded the solution must be equal or less than 1.
For the second case $\beta = 0 \Rightarrow \gamma = \alpha$ we get $\cosh(2\gamma l) = \cosh(2\alpha l)$, which is always greater than 1 ($\cosh(x) \geq 1$).

As a result, based on the values of $\beta_1\beta_2$ we will get either a propagating or a decaying wave, and by so creating an effective band-pass filter.

Dispersion

An important property of a waveguide built from unit cells is its dispersion – the relation between the temporal frequency ω and the spatial frequency k. Considering the voltage or the current along the transmission line as a Bloch wave, we can extract the spatial frequency $k(\omega)$ by scanning the wave along the transmission line with a known periodicity.

From equation 7 we see that in a normal transmission line we would expect to get a linear dispersion. While in the case of metamaterial we would expect to get a nonlinear dispersion relation, as seen in equation 9.

Methods

The measuring system

All of the measurements were taken via vector network analyzer (VNA), two different ways of obtaining data were used:

a. Measuring the transfer coefficient by transmitting waves from one end of the TL to the other.

b. Transmitting waves from one end of the TL to the other while scanning from above with a probe at fixed locations with the help of an engine (see Fig4). The data that was obtained from this measurement is proportional to the wave function of the system.

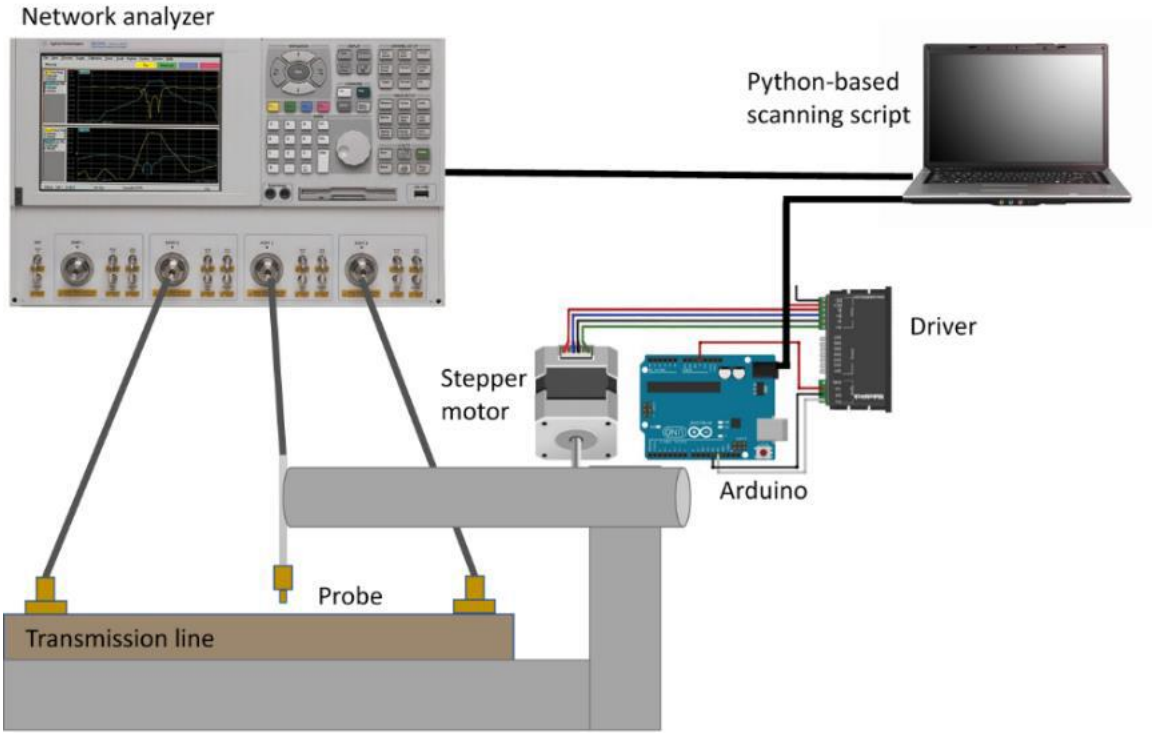

Figure 4 – The experimental system that was used for scanning the TL from above as specified in way b. A stepper motor controlled by an Arduino was moving a probe over fixed positions over the TL. The Arduino was controlled by a python script which also managed the VNA measurements.

About the code and simulations

In order to find the best parameters for the systems used in this experiment we used numerical simulations of the filter TL and CRLH TL. This simulation used the previously mentioned ABCD matrices method to simulate the propagation of microwaves through the TL and to calculate different measurable parameters of the system, such as the frequency dependent transfer coefficient at the end of TL; the wave function over different locations of the TL and at different frequencies; and the dispersion relation of the TL. For further explanations on simulating the wave function see Oppenheim and Rubinstein. The code was written in python and is available on demand. Furthermore, a code for controlling both the Arduino and the VNA was updated and adapted from code provided by Oppenheim and Rubinstein and from Prof. Nadav Katz's Quantum Coherence lab.

Simple filter

In the first part of the experiment we used a 10 cell coplanar waveguide (CPW) filter, in order to validate our ability to simulate transmission lines using ABCD matrices and to calculate the transfer coefficient of the entire TL and its dispersion relation. Our results are shown in Fig5, we see that we were able to simulate the TL in a good way, albeit some differences. We can see, as expected, that the experimental sweep is much noisier than the simulation. Still, from both the simulation and the experiment it can be seen that the 10-cell TL acts as a high pass filter for frequencies above 13GHz. We see that there are differences between the simulation and the experimental results of the transfer coefficient at the end of the line, those can be explained by the fact that the simulation assumes an ideal line with no losses. Oppenheim and Rubinstein were able to include the losses in

their simulation to get better results, which was not attempted for this experiment. Regarding the dispersion relation we got a noisy relation which is linear from 6 GHz in the experimental measurements, while the simulation is indeed liner as expected. Let us note, that extracting the dispersion relation from the experimental data was relatively hard, and it is possible that better measurements or better data cleaning is required in order to get better results.

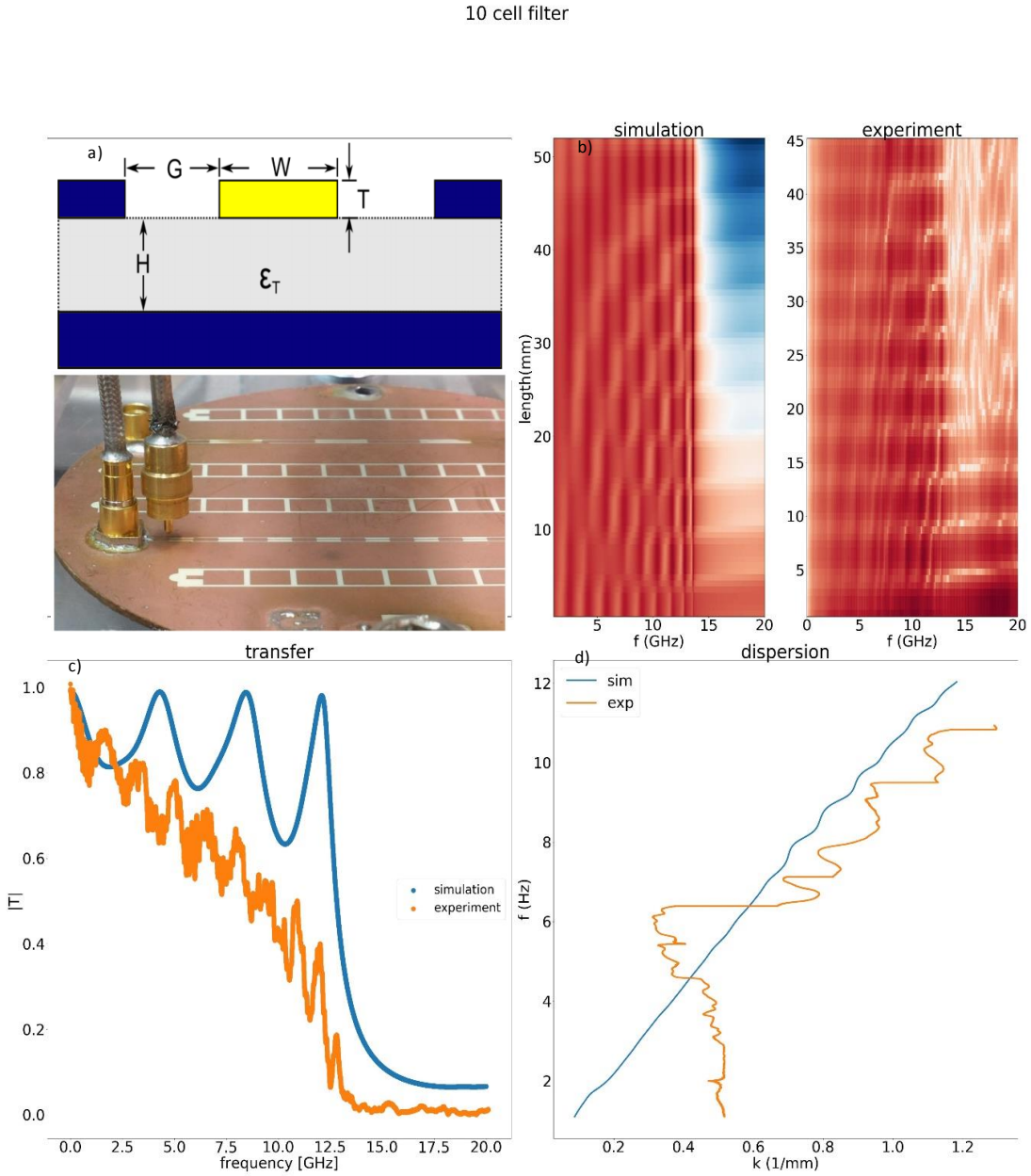

Figure 5 – measurements and simulation of a simple 10 CPW cell filter. a) top – a cross section of a CPW; bottom – a picture of the probe on top of the 10-cell filter, for specific parameters see appendix. b) a sweep of voltage over different positions across the filter at different frequencies. On the left simulation results and on the right the experimental results. c) the transfer coefficient at the end of the filter – simulation and experiment. d) simulation and experimental results of the dispersion relation of the filter, showing linear relation.

Metamaterials

In the second part of the experiment we measured a one mass metamaterial, whose parameters are described in the appendix. We again get that the experimental sweep behaves as predicted by our simulation has some added noise, and less clear band gap. It is worth noting that since we use a probe for the sweep measurements, we expect to get a less clear result. The probe scans from above the line, so the intensity measured is weak and much more prone to disturbances. Furthermore, we have tried to keep the measurement height as constant as possible, but since certain scanning points are above capacitors we get places where the probe is closer to the surface than other places. We would recommend trying to investigate the effect of the height of the probe on the measurements or trying to find a better method of probing the line itself. Also, deeper examination of the pass band before the gap shows further differences between the experimental results and the simulation as can be seen in Fig7.

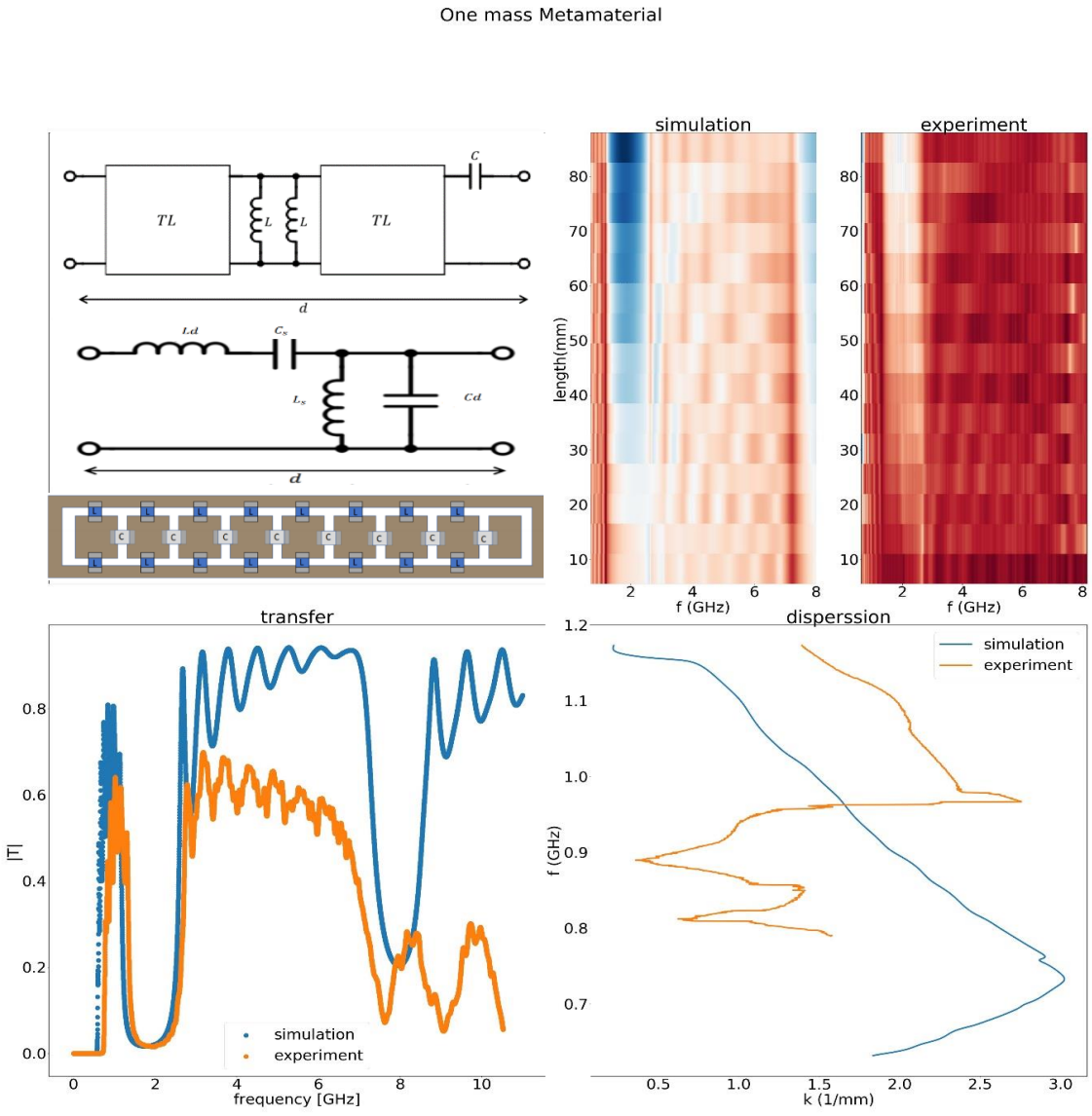

Figure 6 - measurements and simulation of a single mass metamaterial. a) top – a model for each cell in the metamaterial; middle – a lossless circuit model for CRLH-TL; bottom - Illustrated CRLH line (top view): the brown areas are the exposed copper of the CPW. The blue parts are the inductors and the grey parts are the capacitors. b) a sweep of voltage over different positions across the metamaterial at different frequencies. On the left simulation results and on the right the experimental results. c) the transfer coefficient at the end of the metamaterial – simulation and experiment. d) simulation and experimental results of the dispersion relation of the metamaterial, showing nonlinear dispersion relation.

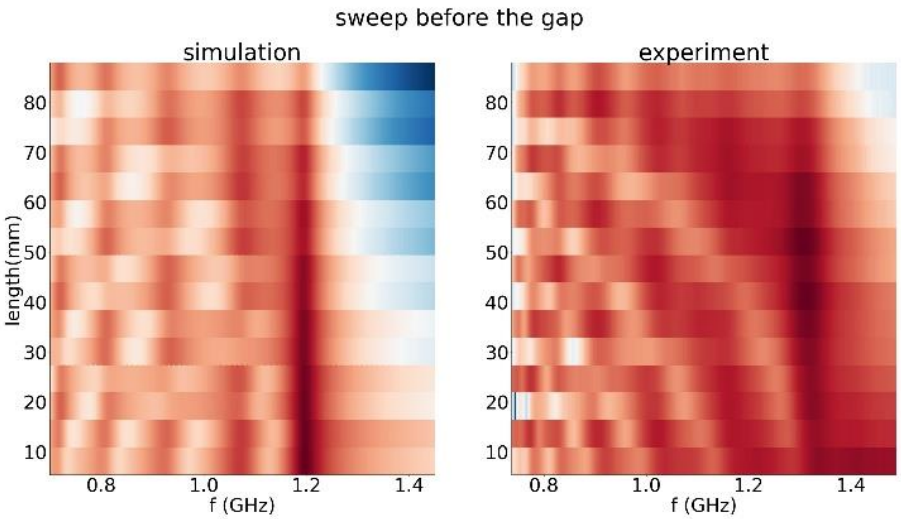

Figure 7 – a comparison of the pass band before the gap between the simulation and the experiment. we see that the experimental results behave differently from the simulation, which might explain the drift in the dispersion relation

We have not investigated those differences, and it might be interesting to understand them.
Even with the differences mentioned above, we still see that the transfer coefficient of the entire line fits the simulation. In order to get a more accurate simulation we used Oppenheim's and Rubinstein's added shunt capacity arising from the gaps in the CPW on top of which the capacitors and inductors are placed on. In both the simulation and the experimental data we get a nonlinear dispersion relation for the line, although here again we get different results, that may occur from the differences in the first pass band which was used to extract this dispersion relation. As mentioned in the theory section, the band gap size is equal to twice the size of the metamaterials mass, and we indeed get a good result which agrees with the theory as shown in fig6c.

Comparison of between a Defect and a topological state

Wei et. al shown that a topological local state is created when taking two opposite masses metamaterials [1]. This state is located in the meeting point of both these masses and is highly localized. We also know that impurities and defects in periodic structures induce local states in the defects themselves. We then tried to measure and compare the behavior of a topological state induced in the boundary of two different masses metamaterials of the same size to the behavior of a defect created in the one mass metamaterial previously mentioned. We used the two mass metamaterial TL used by Oppenheim and Rubinstein [2] as described in the appendix. We then created a one mass metamaterial TL similar to the one in the previous section and switched the inductors in the fifth cell to a 2nH inductors. We chose those inductors after running several simulations with different defects and defect positions on the line in search for a local state created in the bang gap of the one mass metamaterial. We got that on our system the best local state is induced by 2.5nH inductors in the fifth cells as a defect. We used instead the 2nH inductors in lack of 2.5nH inductors, which still gave a clear local state in the band gap of the one mass metamaterial. We then measured both systems, as seen in Fig8, on both systems a local state appears in the band gap of the one mass metamaterial as can be seen in the second row of the figure We see that both the topological state and the defect induced local state behave similarly. We do notice slight differences between the two states.
First, as seen in the first and last row of Fig8, the defect induced state is more localized around the

defect than the topological state around the boundary. Second, the topological state is slightly more intense locally as seen in the last row, while the defect induced state appears to be not insignificant over the entire TL as can be seen in the middle row. It is also worth noticing, that the behavior of other frequencies over the boundary\defect is different. While over the defect only the bound state frequency is significant, over the boundary we get another state around 3GHz. It is also noticeable that general behavior of the entire line is significantly different, which is to be expected.

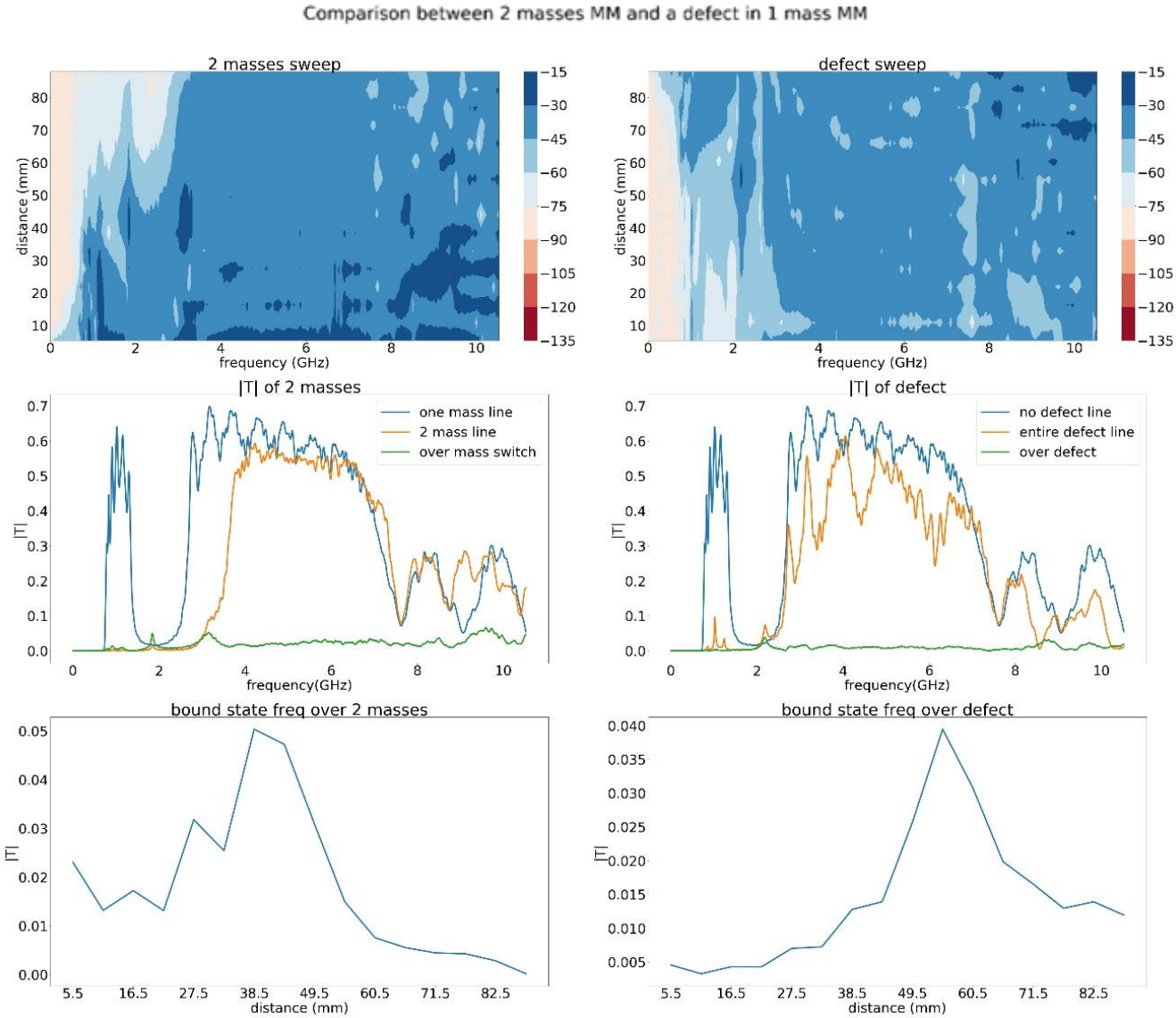

Figure 8 - A comparison between the experimental behavior of a topological state induced by 2 masses (on the left column) and a local state induced by a defect (on the right column) created by switching one set of inducers in the one mass metamaterial of section B with 2nH inducers in the 5th cell. Top row – a comparison of the sweeps, the local state is visible on both cases near the 2GHz frequency. Middle row – the transfer coefficient of the tested material at the end of the line and over the interest point in comparison to the regular 1 mass metamaterial, the local state is visible on both cases. Bottom row – a comparison of the transfer coefficient over all the measurements points along the lines in the bound state frequency.

Since differentiating between a real topological state to a non-topological state is an important mission, we wanted to see if we can find other characteristics in which the topological state and the defect induced state differ from each other. We tried to see if the defect is location sensitive and

compare its behavior in different locations to moving the boundary between the two masses. This was only done numerically, and the results are shown in Fig9. We have chosen five different locations for the defect\masses boundary and simulated the transfer coefficient at the end of each line, as well as the transfer coefficient over the boundary\defect and the sweep at the local state frequency over the entire line. The results show that both types of local states are not significantly influenced by the position of the defect\boundary, and that both of them remain very stable in all of the simulations. In summary, we see that although there are slight differences between the behavior of the topological state and the defect induced state, they are very similar and might not be as easy to differentiate using the measurements and simulations done in this experiment. In the discussion section we shall show more numerical work done to try and find differences and suggest further experiments to be conducted using these two systems.

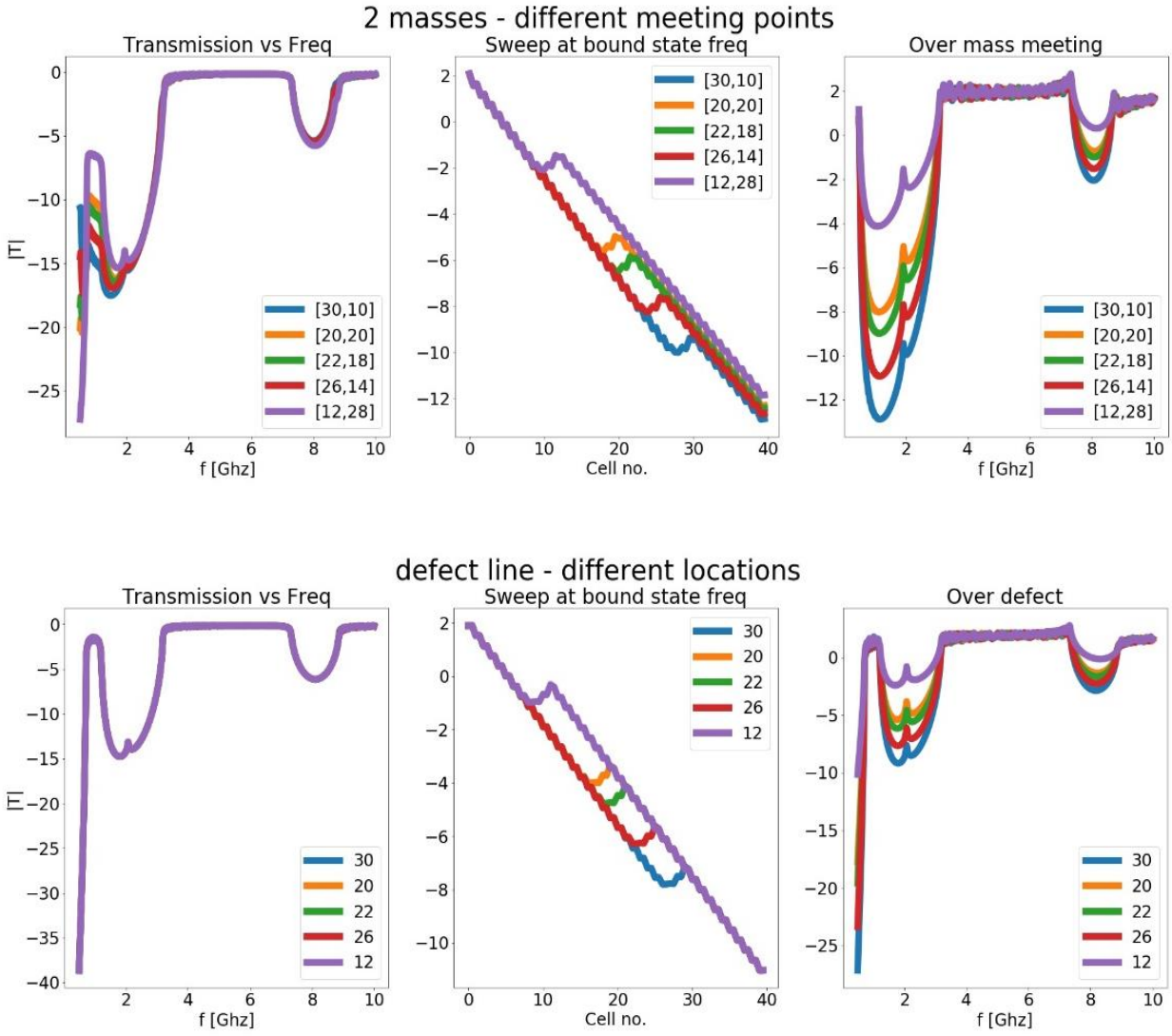

Figure 9 – a comparison of the effects of moving the masses border in the 2 masees line and the defect in the 1 mass line. Each color stands for a different location. It is shwon that both the topological state and the defect induced state are independent of their location inside the line. All graphs are in log scale

Discussion

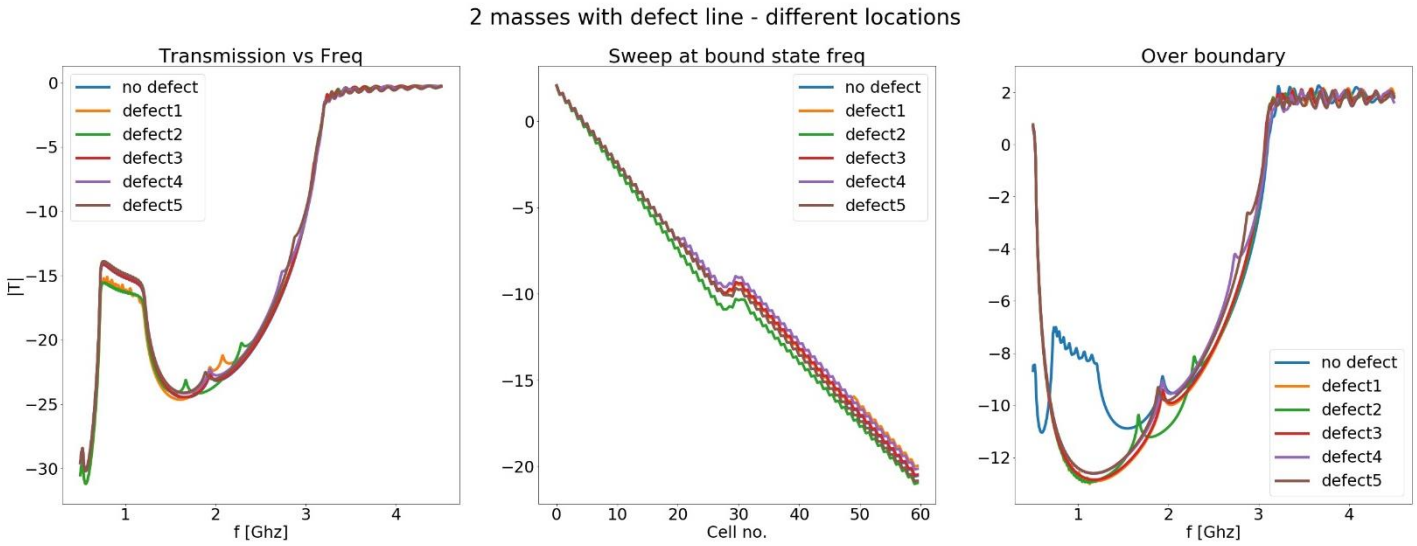

Figure 10 – Numerical simulation of 2 masses CRLH TL made of 60 cells, 30 of each mass, in the presence of defects. The defect introduced is again a swap of two inductors in a single cell. The defects vary in position along the line and in type of inductors and are available in the appendix. Left - the transfer coefficient at the end of the entire line. Middle – the transfer coefficient over the entire line in the local state frequency. Right – the transfer coefficient over the mass boundry. All the graphs are in log scale.

So far, we have seen that one can simulate the properties of a 1D transmission line using the ABCD matrices method. Furthermore, we saw that the theory of CRLH TL fits the experimental behavior of these systems. We also saw that a topological state is indeed created as predicted in the boundary of two masses CLRH TL. We then demonstrated that this topological state is similar to a state induced by a defect in a one mass CLRH TL. Experimentally, we have shown the measurements of the defected one mass metamaterial and comparison to the 2 masses TL and witnessed their resemblance. Numerically, we have shown the location independence of these local states.

Since all of our measurements and simulations revealed the high similarity between the topological state and the defect induced state, we have decided to try and investigate the stability of the topological state while being exposed to defects in the line. We know that defects are extremely sensitive to the appearance of more defects, and we wanted to test if the topological system would be as sensitive. This was also done purely numerically, for lack of time to produce all the different TL needed. The results can be seen in Fig10 where we tried to add different defects to the 2 masses CRLH TL we used in the experiment. The results indeed show that the state cannot be destroyed using the defects we have introduced, while we know that the defect induced state is destructible by adding other defects to the line. Even though we didn't find a way to destruct the topological state, we do see that the state is indeed influenced by the appearance of specific types of defects in the line, specifically we managed by introducing defect2 to substantially move the frequency of the state and also to create another allowed state in the band gap. We would recommend further exploring the difference between the two types of states, both by experimentally measuring the different simulations we have shown in this section and expanding on them by adding more defect to the two masses TL and testing further types of defects. Apart from that we would recommend looking into other aspects of the measurements we have not, such as the phase and the return coefficient.

To conclude, we were able to measure a topological state created by a boundary between to different and opposite mass CRLH TL and compare it to a defect induced local state. We have shown both numerically and experimentally that these states are similar in their behavior but has started

investigating into potential differences that require further work. We would like to thank Tom Dvir for his guidance and support during this experiment. We would also like to thank Prof. Nadav Katz for his support and for providing us the infrastructure and facilities for this experiment.

Appendix

The experimental systems

In this experiment we used 4 different setups of TL. The different parameters of the systems are as follows:

10-cell filter

This filter was fabricated on a Rogers with the following parameters:

ϵT = 3.5

$H = 0.75 \cdot 10^{-3}\ [m]$

$T = 10 \cdot 10^{-6}\ [m]$

On the surface of the Rogers board there were two CPW, created by lithography.

For the first CPW: $W1 = 100 \cdot 10^{-6}\ [m]$; $G1 = 550 \cdot 10^{-6}\ [m]$

For the second CPW: $W2 = 750 \cdot 10^{-6}\ [m]$; $G2 = 230 \cdot 10^{-6}\ [m]$

Each CPW was of length $6.6 \cdot 10^{-3}\ [m]$

CRLH TL

All the CRLH TL were constructed on top of a PCB with the following parameters:

The CPW dimensions of a single cell were:

$W_{CRLH} = 3 \cdot 10^{-3}\ [m]$; $G_{CRLH} = 0.5 \cdot 10^{-3}\ [m]$; $l = 11 \cdot 10^{-3}\ [m]$

And the gap between two CPW's was: $g = 0.5 \cdot 10^{-3}\ [m]$

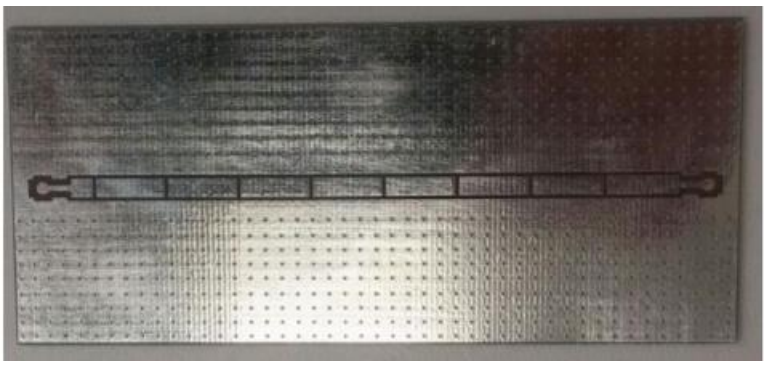

The PCB on top of which all the CRLH TL were constructed

One mass metamaterial

Each cell of this CRLH was built with 1 capacitor and inductors with the following parameters:

$C_s = 1pF; L_s = 15nH$

The system is as described on the bottom of fig6a and consists 8 cells.

2 masses metamaterial

This CRLH TL was created by creating 2 sets of 4 cells on top of the above PCB, each with a different set capacitors and inductors.

The first set is the same as the one mass above $C_s = 1pF; L_s = 15nH$

The second set is made of $C_s = 43pF; L_s = 2nH$

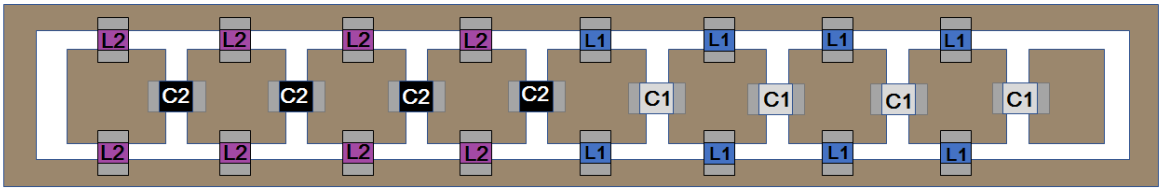

A top view of the 2 masses CRLH TL

One mass metamaterial with defect

This CRLH TL was created by taking the same design of the One mass TL and replacing both the inductors in the fifth cell with $L_s = 2nH$ inductors

Defects induced in figure 10

The simulation consisted of a 2 masses metamaterial made of 30 CRLH cells of the first set of capacitor and inductors that was used in this experiment connected to 30 CRLH cells made of the second set of capacitor and inductors used. This was used as the 'no defect' line. the defects introduced are as follows:

defect1 – the inductors in cell 11 were changed to $2.5 \cdot 10^{-9}nH$

defect2 – the inductors in cell 29 were changed to $2.5 \cdot 10^{-9}nH$

defect3 – the inductors in cell 40 were changed to $2.5 \cdot 10^{-9}nH$

defect4 – the inductors in cell 40 were changed to $12.5 \cdot 10^{-9}nH$

defect5 – the inductors in cell 31 were changed to $12.5 \cdot 10^{-9}nH$

Bibliography

[1] T. Wei, S. Yong, C. Hong and S. Shun-Qing, "Photonic simulation of topological excitations in metamaterials," *Sceintific Reports,* 2014.

[2] L. Oppenheim and Y. Rubinstein, "Metamaterials as a window to Dirac equation," 2018.

[3] David.M.Pozar, Microwave Engineering, 1990.

[4] C. &. T. C, Electromagnetic metamaterials: transmission line theory and microwave applications - The engineering approach, 2006, pp. 62-63.